Molecular Vision 2006; 12:467-77 <http://www.molvis.org/molvis/v12/a54/>
Received 24 January 2005 | Accepted 10 April 2006 | Published 10 May 2006

Microglia and macrophages are increased in response to ischemia-induced retinopathy in the mouse retina

Michael H. Davies, Joshua P. Eubanks, Michael R. Powers

Department of Pediatrics, Casey Eye Institute, Oregon Health and Science University, Portland, OR

Purpose: The ability of microgilal cells (MG) and macrophages (MAC) to release cytokines, induce apoptosis, as well as perform phagocytic functions suggests a possible role in wound healing following oxygen-induced injury. This study was performed to determine the temporal and spatial expression of F4/80 (F4/80$^+$) positive microglia/macrophages (MG/MAC) in areas of retinal damage in the mouse model of oxygen-induced retinopathy.

Methods: C57BL/6 postnatal day 7 (P7) mice were exposed to 75% O_2 for 5 days (P12) then allowed to recover in room air. Hyperoxia-exposed (O_2) mice (O_2 refers to hyperoxia exposure from P7 to P12 only) were sacrificed on P12, P14, P17, and P21 and their eyes were examined. Localization of F4/80$^+$ cells in FITC-dextran-perfused retinas allowed coordinate visualization of retinal vessels and MG/MAC via fluorescence microscopy. BrdU, a cellular proliferation marker, was injected intraperitoneally 1 h prior to sacrifice. Immunostaining was performed for a microglia and macrophage-specific antigen (F4/80) and BrdU. CCL2 (monocyte chemoattractant protein-1; MCP-1) expression was examined by quantitative real time reverse transcriptase polymerase chain reaction (RT-PCR).

Results: There was a marked increase (>500%) in MG/MAC in hyperoxia-exposed retinas on P17O_2 and P21O_2 compared to control retinas. At P17O_2, MG/MAC were localized in areas of neovascularization (NV), revealing an intimate relationship between MG/MAC and neovascular tufts. However, P21O_2 retinas demonstrated MG/MAC associated with avascular regions in the outer layers of the retina. Immunostaining for F4/80 and BrdU revealed rare co-localization in hyperoxia-exposed retinas. Real time RT-PCR results demonstrated increased expression of CCL2 in P14O_2- and P17O_2-exposed retinas.

Conclusions: Our results suggest that resident retinal microglia proliferation occurs at a low frequency in response to injury in this model. The substantial increase in total F4/80$^+$ cells in hyperoxia-exposed retinas in conjunction with the upregulation of CCL2 is consistent with recruitment of hematogenous macrophages into the retina. The temporal and spatial localization of MG/MAC adjacent to neovascular tufts suggests these cells are modulating the retinal response to ischemia-induced retinopathy.

Retinopathy of prematurity (ROP) was first described in 1942 and continues to be a major clinical issue for the ophthalmologist [1]. Advances in neonatal care have increased the survival of small infants under 26 weeks of gestation, but these same infants are at highest risk for developing ROP [2]. Significant retinal neovascularization (NV) and retinal detachment characterize the severe form of ROP, although less severe manifestations of the disease exist, which can also spontaneously regress [1]. Animal models of oxygen-induced retinopathy have permitted the study of this pathological disease process, with a major focus on the retinal cytokine response to ischemia-induced injury [3,4]. It has become apparent that pathologic angiogenesis is a complex process involving several angiogenic growth factors, proteases, and adhesion molecules [5]. Although (VEGF) is a key player in retinal NV, various other angiogenic growth factors contribute to this process, including but not limited to, insulin-like growth factor (IGF-1), angiopoietin 1, and angiopoietin 2 (Ang-1, Ang-2), and placental growth factor (PlGF) [6-8]. Recent reports have also shown that retinal cell apoptosis via the Fas/Fas-ligand pathway can play a counterbalance role to the pro-angiogenic effects of these growth factors, leading to vascular tuft regression and thereby modulating pathologic NV [9,10].

Microglia and macrophages are two cell populations that have the potential to contribute to both retinal NV and vascular tuft regression. Microglia precursors enter the developing retina and are involved in phagocytosis of dying neurons during retinal development [11,12]. Microglia become quiescent in the postnatal period but become activated in response to injury or inflammation [11]. In contrast, hematogenous macrophages are recruited to retina by inflammatory chemokines in response to injury [13]. Chemokines are a family of peptides that activate and attract leukocytes to sites of inflammation and infection [14]. Chemokines have also been shown to be capable of directly mediating angiogenesis and hematopoiesis [15]. In addition, several in vivo studies have revealed that despite redundancy with other chemokines in vitro, CCL2 (MCP-1; monocyte cheomattractant protein-1) is the major chemokine responsible for macrophage influx in several injury models [16-18].

Macrophages are capable of releasing angiogenic cytokines and known to contribute to inflammatory NV, tumor angiogenesis, and choroidal NV [19-22]. Microglia and

Correspondence to: Michael R. Powers, MD, Casey Eye Institute, Oregon Health and Science University, Mail Code L467IM, 3181 SW Sam Jackson Park Road, Portland, OR, 97239; Phone: (503) 494-8023; FAX: (503) 494-6875; email: powersm@ohsu.edu

macrophages have also been linked to retinal injury in models of diabetic and ischemic-induced retinopathies [23,24]. Depending on the microenvironment, these cells are also capable of mediating endothelial cell (EC) death via initiation of the caspase cascade of apoptosis [25-28]. These cells can also play a phagocytic role and are activated and recruited to regions of retinal and brain injury [29-31].

To further characterize the role microglia and macrophages play in retinal NV and vascular tuft regression, we used a mouse model of oxygen-induced retinopathy. This model reproducibly develops preretinal NV anterior to the inner limiting membrane. Additionally, this disease model is characterized by the predictable regression of neovascular tufts via apoptosis [3,10]. These studies describe the temporal and spatial distribution of microglia and macrophages in retinas with ischemic retinopathy, supporting an important role for these cells in both the phase of NV and vascular tuft regression.

METHODS

Animals: Untimed pregnant C57BL/6 (B6) mice were obtained on post-conception day 15 from Jackson Laboratories (Bar Harbor, ME). Mice were housed in the Oregon Health and Science University animal care facilities and treated in accordance with National Institute of Health (NIH) guidelines and the guidelines of the ARVO statement for the Use of Animals in Ophthalmic and Vision Research. Using the mouse model of oxygen-induced retinopathy established by Smith et al. [3], postnatal day 7 (P7) mice, along with nursing females, were exposed to 75%±2% oxygen for 5 days and then allowed to recover in room air on P12. Room air control mice were raised under identical light and temperature conditions. Mice were sacrificed on P12, P14, P17, P21, and P24 by CO_2 euthanasia or cervical dislocation. Eyes were enucleated and processed for histological studies or RNA isolation and analysis. Subsets of eyes were used in retinal flat-mount studies, including fluorescein angiography as described in the next section below.

Fluorescein angiography: Fluorescein angiography was performed on P17 and P21 for qualitative assessment of the retinal vasculature and for coordinate visualization with F4/80-immunolabeled cells [32]. Briefly, mice were deeply anesthetized via a subcutaneous injection of a cocktail containing ketamine, xylazine, and acepromazine, 3 µl/g of body weight. Mice were then perfused through the left ventricle with 1 ml of a PBS solution containing 50 mg high molecular weight ($2x10^6$) FITC conjugated dextran (Sigma, St. Louis, MO).

Assessment of retinal microglia and macrophages: For retinal flat-mount studies, a small incision at the limbus of the enucleated eye was made to cut away the cornea and iris. Then fine tip forceps were used to peel away the sclera, leaving the retina around the lens. After an initial fixation in 4% paraformaldehyde (PFA) for 3 h at 4 °C the lens was removed in such a way that the retina maintains the globe shape. It was then fixed for an additional 21 h at 4 °C. Following fixation, retinas were washed with dH_2O and treated with 0.001% trypsin for 5 min at room temperature (RT). Followingtris-buffered saline (TBS) washes, retinas were incubated in 2% rabbit serum for 3 h. Rat antimouse F4/80 antigen antibody (Serotec, Raleigh, NC) was diluted in 2% rabbit serum to a concentration of 0.11 mg/ml. This antibody has been well characterized in its specificity for mouse microglia and macrophages [33]. Retinas were incubated in antibody solution for 36-48 h at 4 °C. Following extensive washing in TBS, retinas were then incubated with a biotinylated rabbit antirat mouse-absorbed IgG (Vector Laboratories, Burlingame, CA). ABC-AP kit (Vector) was then applied to retinas and visualized via Fast Red (BioGenex Laboratories, San Ramon, CA). Substrate development was quenched with dH_2O and stained retinas were fixed for 24 h in 4% PFA at 4 °C. Retinas were then dissected free of vitreous to remove any associated hyalocytes and flat-mounted on SuperFrost® Plus coated slides (Fisher Scientific, Pittsburgh, PA) under a coverslip with SlowFade® (Molecular Probes, Eugene, OR) as the mounting media. Quantification of microglia and macrophages (MG/MAC) was carried out via light microscopy in a masked fashion. A micrometer disc with a grid of 20x20 on a 1 cm square was put into a 10x eyepiece and placed onto a binocular microscope with a 10x objective. A Lovins Micro-Slide Field Finder (Gurley Precision Instruments, Troy, NY) was positioned on the microscope stage, atop of which was placed a slide containing a flat-mounted retina immunohistochemically stained for F4/80 antigen. The microscope was focused through the retina onto the Field Finder slide (Gurley), and the grid of the micrometer disc was aligned with the numbered grid on the slide. The microscope was then focused up to the superficial (vitreal) retina, and MG/MAC located within the confines of the micrometer disc were counted. We then focused on deeper areas of the retina and again counted MG/MAC that were within the confines of the micrometer disc. Finally, the amount of the micrometer disc grid that was occupied with retinal tissue was counted to determine total area of retinal tissue examined. This procedure was followed until the entire retina was examined. Retinas from room air control and hyperoxia-exposed mice were quantified for $F4/80^+$ cells as previously described from P12, P14, P17, and P21 (n=3 per time for control retinas, n=4 per time for hyperoxia-exposed retinas).

For coordinate visualization of MG/MAC and the retinal vasculature, FITC-dextran perfused retinas were immunolabeled with rat antimouse F4/80 antibody as previously described. Retinas were flat-mounted on Superfrost® Plus-coated slides under a coverslip with SlowFade® as the mounting media. The retinas were analyzed via fluorescent microscopy and photographed on Ektachrome 160T slide film (Eastman Kodak, Rochester, NY).

Immunohistochemistry: Eyes obtained for immunohistochemistry studies were placed in 10% neutral-buffered formalin (NBF) overnight and routinely processed for paraffin embedding. The eyes were sectioned at 5 µm intervals and placed on SuperFrost® Plus coated slides. Sections were deparaffinized with xylene followed by rehydration in washes of diminishing ethanol concentrations ending with dH_2O. Antigen retrieval was performed by proteolytic digestion with 0.1% trypsin (Sigma) for 5 min then washed in TBS. Subsequently, sections were incubated in a 2% rabbit block for 1 h

at RT in a humidifying chamber. Sections were incubated overnight at 4 °C with F4/80 antibody, diluted to a protein concentration of 0.55 mg/mL in blocking solution. Following TBS washes, sections were incubated with a biotinylated rabbit anti-rat mouse absorbed antibody (Vector) for 1 h at RT. ABC-AP (Vector) system was used to localize antigen. Fast Red (Biogenex) was used as the substrate and reaction was quenched by dH_2O.

In order to determine if F4/80 positive cells were undergoing proliferation, a subset of mice were injected with BrdU for double-labeling of proliferating cell nuclei and $F4/80^+$ cells. Briefly, 25 mg/mL BrdU and 5 mg/ml FrdU were dissolved in a carbonate buffer composed of 0.01 M Na_2CO_3, 0.01 M $NaHCO_3$, 0.1 M NaCl, (pH 9.5). BrdU incorporation is improved by blocking native thymidine synthesis with FrdU [34]. Five μl/g animal body weight of BrdU solution was injected intraperitoneally one hour prior to sacrifice by CO_2 euthanasia. Eyes were then routinely harvested and fixed overnight in 10% NBF. Sections of the BrdU injected eyes were then immunolabeled for F4/80 as previously described. After staining for F4/80 was completed, slides were placed into a glass container and immersed in 0.01 M citrate buffer (pH=6.0). Slides were then boiled 10 min in the microwave for DNA denaturation to allow recovery of BrdU antigen. Anti-BrdU (Dako, Carpinteria, CA) antibody was used to label proliferating cell nuclei using a standard two step immunohistochemical staining protocol and visualized with DAB (Sigma). Slides were counterstained with hematoxylin and mounted with Crystal Mount™ (Biomeda, Foster City, CA).

Reverse transcriptase polymerase chain reaction analysis of cytokines and chemokines: Retinas were dissected on P12, P14, P17, P21, and P24 from room air- and hyperoxia-exposed mice and pooled (n=4) for RNA analysis. RNA was extracted using a one-step guanidine-isothiocyanate protocol [35]. Total RNA was further purified by DNase treatment to remove potential genomic DNA contamination, and then re-isolated by the guanidinium single step method. cDNA was then synthesized using oligo(dT)-primed M-MLV reverse transcriptase (Promega, Madison, WI) for 2 h at 37 °C. Traditional RT-PCR was used to analyze the expression of macrophage colony-stimulating factor (MCSF), granulocyte-macrophage colony-stimulating factor (GM-CSF), and CCL2. Relative mRNA expression of CCL2 normalized to β-actin was further quantified in triplicate by real time PCR using the Chromo4 thermocycler (MJ Research) and iQ™ SYBR® Green supermix (Bio-Rad). RT reaction mixtures were applied to the Chromo4 and amplified with a precycling hold at 95 °C 10 min, followed by 40 cycles of denaturation at 95 °C for 30 s, annealing at 64 °C for 30 s, and extension at 72 °C for 45 s. At the end of each cycle, there was a 1 s hold at 82 °C followed by a plate read for analysis using the Chromo4 Opticon Monitor 2 software. Annealing temperatures and read temperatures were pre-determined using control mRNA. Melting curves were run after product formation, and samples were run on a 2.5% agarose gel to confirm product size. The mouse specific primer sets were synthesized by Integrated DNA Technologies, Inc. (IDT, Coralville, IA) with the following sequences: CCL2, 5'-GGC TGG AGA GCT ACA AGA GGA TCA-3' and 5'-GGC ATC ACA GTC CGA GTC ACA CTA-3', GM-CSF, 5'-TGG AAG CAT GTA GAG GCC ATC AA-3' and 5'-GGC TCA TTA CGC AGG CAC AA-3', M-CSF, 5'-CCA TTG GCC AGA CAC AGA ATT A-3' and 5'-GCT CCT CCA CTT CCA CTT GTA GAA C-3'. A primer pair for the constitutively expressed β-actin gene was included in each assay as an internal loading control (Sense: 5'-ATG CCA ACA CAG TGC TGT CT-3'; Antisense: 5'-AAG CAC TTG CGG TGC ACG AT-3'; IDT). PCR products were separated via gel electrophoresis and photographed under ultraviolet illumination.

RESULTS

Increased microglia and macrophages in ischemic retinas: Fluorescein angiography of retinal whole mounts of P17 room air control B6 mice (Figure 1A) demonstrates normal vasculature compared to P17 hyperoxia-exposed (O_2; O_2 refers to hyperoxia exposure from P7 to P12 only) retinas (Figure 1B), which revealed avascular regions and neovascular tufts. Whole-mount immunohistochemical staining for F4/80 antigen on P17 control retinas (Figure 1C) showed positive cells located diffusely throughout the retina. In contrast, $P17O_2$ retinas revealed a substantial increase in MG/MAC numbers as a result of ischemic injury (Figure 1D). This increase was observed throughout the retina but primarily at the transition between vascular and avascular retina. Higher magnification of P17 room air control (Figure 1E) and $P17O_2$ (Figure 1F) retinas revealed not only increased density of MG/MAC in the hyperoxia-injured retinas, but also a more reactive morphology. In addition, there appeared to be increased numbers of amoeboid microglia as well as infiltrating monocytes and macrophages.

To quantify this apparent increase in microglia/macrophages, we counted total $F4/80^+$ cells as well as total retinal area to determine the number of MG/MAC per millimeter square of retinal tissue ($F4/80^+/mm^2$). We found that control retinas from all times had a relatively constant amount of resident microglial cells, a mean of 28.98±5.44 $F4/80^+/mm^2$. When hyperoxia-exposed retinas were examined, we found that MG/MAC numbers were not significantly altered on $P12O_2$ and $P14O_2$. However, there was a significant increase in retinal MG/MAC on $P17O_2$, 155.5±17.12 $F4/80^+/mm^2$ ($p<0.001$), and on $P21O_2$, 237.25±43.21 $F4/80^+/mm^2$ ($p<0.001$; Figure 2).

Retinal microglia and macrophage localization during neovascularization: Immunohistochemical localization of F4/80 in retinal cross-sections and fluorescein-perfused retinas allowed us to determine MG/MAC locations within the normal and hyperoxia-injured retinas. P12 room air control retinas revealed $F4/80^+$ cells localized along the inner plexiform layer (IPL) and outer plexiform layer (OPL; arrowhead, Figure 3A) as previously published [36]. Note the $F4/80^+$ cell surrounding a pyknotic nuclei in the inner nuclear layer (INL; Figure 3A, arrow and insert). $P12O_2$ retinas had a similar staining pattern as the room air control retinas (Figure 3B; OPL, arrowhead), although there appeared to be more $F4/80^+$ cells along the nerve fiber layer (Figure 3B, asterisk). Again, note

the pyknotic nuclei in the INL (Figure 3B, arrow and insert). On P14 and P14O_2, retinas continued to have F4/80$^+$ cells located in the IPL (arrow) and OPL (arrowhead) of the retina (Figure 3C,D). However, P14O_2 retinas continued to exhibit F4/80$^+$ cells along the nerve fiber layer (Figure 3D, asterisk). On P17, F4/80$^+$ cells could still be found in both the plexiform layers of the room air control retinas but appeared to be less reactive and more ramified than earlier times (Figure 3E, arrow, IPL, arrowhead, OPL). In contrast, in P17O_2 retinas the F4/80$^+$ cells appeared to have migrated from the plexiform layers into the region of the preretinal neovascular tufts (Figure 3F, arrows). Fluorescein angiography further demonstrated that on P17O_2, F4/80$^+$ cells were primarily associated with the regions of NV as observed by the intimate relationship between MG/MAC and neovascular tufts (Figure 3G, arrows). Fluorescein angiography in room air control retinas on P17 exhibited F4/80$^+$ cells in a diffuse pattern (data not shown).

In the P21O_2 retina, the vascular pattern remained similar to that which was seen at P17O_2, including avascular regions (Figure 4A, asterisk). F4/80$^+$ cells continue to be localized along the vascular and avascular transition areas. While neovascular tufts were less prevalent on P21O_2, those that remained still demonstrated a close relationship with F4/80$^+$ cells (Figure 4A,B, arrows). In addition to those F4/80$^+$ cells found

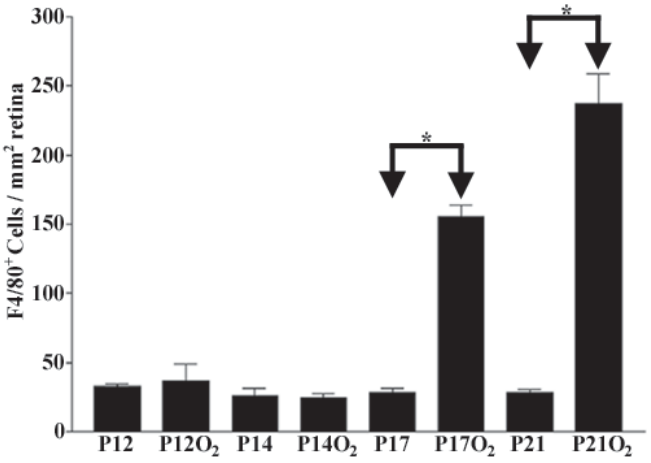

Figure 2. Quantification of retinal microglia and macrophages in oxygen-induced retinopathy. F4/80$^+$ cell numbers increased on P17O_2 and P21O_2 compared to age-matched room air controls (O_2 refers to hyperoxia exposure from P7 to P12 only). Cell numbers remained constant at all other times and conditions examined. Asterisk indicates p<0.001 by one-way ANOVA followed by the Tukey's post-test.

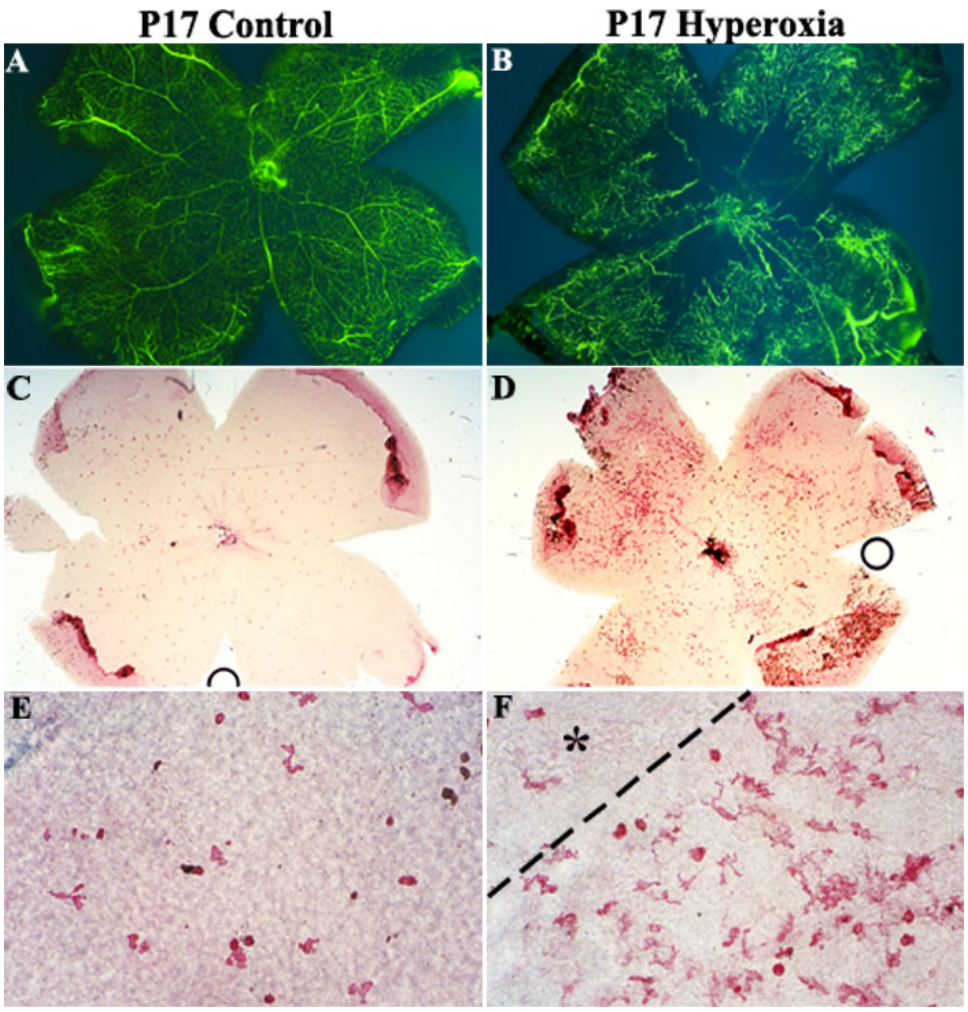

Figure 1. Immunolabeled F4/80 cells in retinal flat mounts. Fluorescence angiography showed retinal vasculature in B6 mice on P17 room air (**A**) compared to P17 Hyperoxia mice (**B**). Immunohistochemical localization of F4/80$^+$ cells in P17 control retinas (**C**) compared to P17 Hyperoxia retinas (**D**). Higher magnification of F4/80$^+$ cells in P17 control (**E**) and P17 Hyperoxia (**F**) retinas revealed not only an increased number of microglia/macrophages but also more activated microglia with multiple processes. Dashed line (**F**) denotes the transition region between avascular (asterisk) and vascular retina where neovascularization is known to occur. Magnification 25x (**A**-**D**); 400x (**E**-**F**).

in the superficial vascular network on P21O_2 (Figure 4C,E), we also found groups of MG/MAC associated with avascular regions at or below the level of the deep retinal vasculature in the hyperoxia-injured retinas (Figure 4D,F, arrows).

Retinal cell proliferation in oxygen-induced retinopathy: To determine if the increased number of retinal MG/MAC in the hyperoxia-injured retinas was secondary to proliferation, immunohistochemistry was used to co-localize F4/80$^+$ cells with BrdU in retinal cross-sections. We found that on P14 the room air control retinas showed few positive BrdU cells (data not shown), while the hyperoxia-exposed retinas demonstrated proliferating cells along the inner regions of the retina on P14O_2

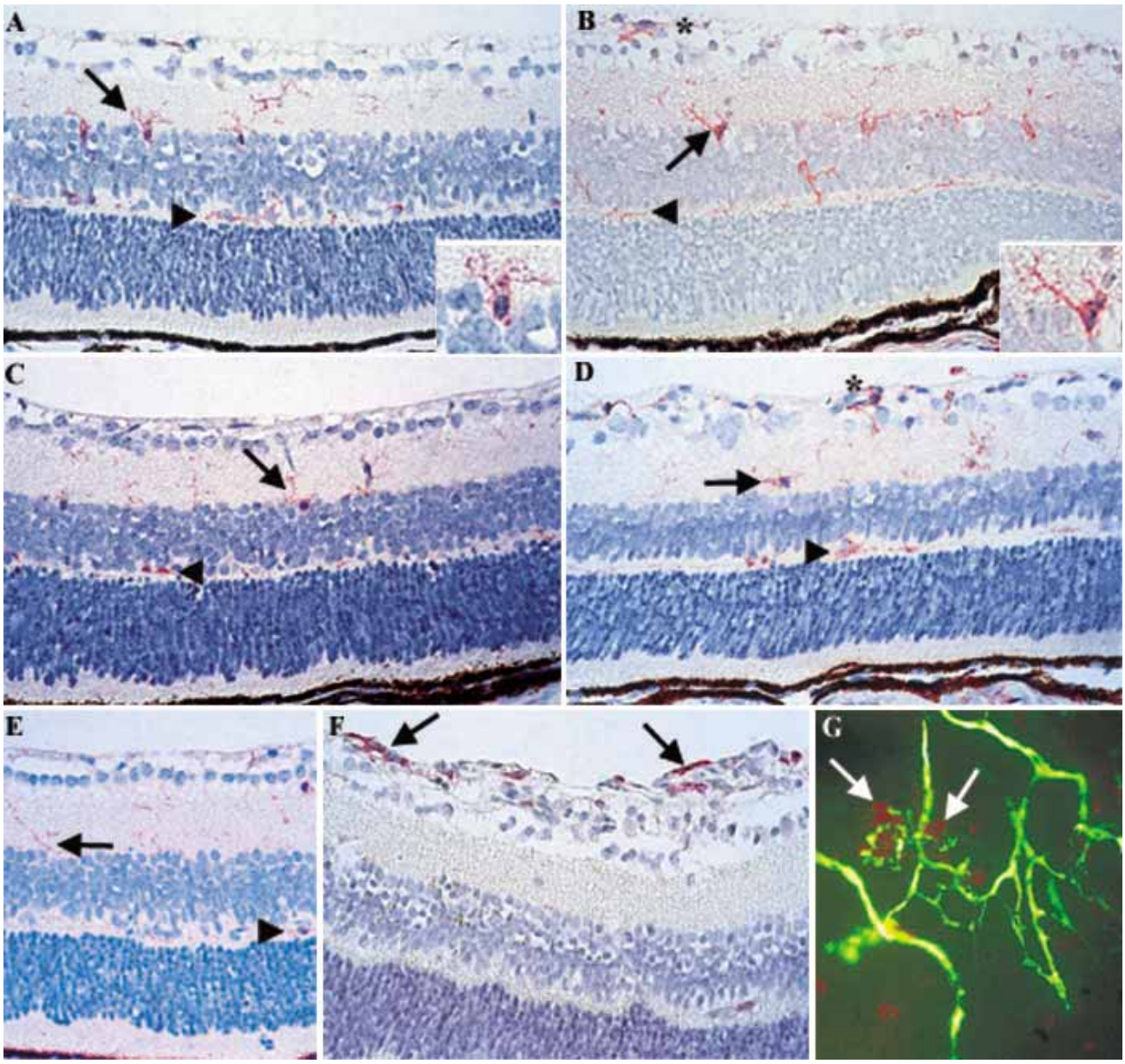

Figure 3. Localization of microglia and macrophages in oxygen-induced retinopathy. **A**: Immunostaining for F4/80 in P12 room air retinas revealed F4/80$^+$ cells (red) along the inner plexiform layer (IPL; arrow) and outer plexiform layer (OPL; arrowhead). F4/80$^+$ cells located in the IPL (arrow) are seen around pyknotic nuclei (insert). **B**: P12O_2 retinas showed a similar staining pattern with cells along both the IPL (arrow) and OPL (arrowhead), with additional cells along the nerve fiber layer (NFL, asterisk). As with P12 room air- control retinas, F4/80$^+$ staining is localized to pyknotic cells (insert) located in the IPL (arrow). **C**: P14 control retinas have comparable staining to P12 room air-retinas (IPL, arrow; OPL, arrowhead). **D**: Following oxygen-induced injury, P14O_2 retinas demonstrated increased F4/80$^+$ cells along the NFL (asterisk) in addition to those cells found in the IPL (arrow) and OPL (arrowhead). **E**: P17 room air controls have slightly less activated F4/80$^+$ cells still localized to the IPL (arrow) and OPL (arrowhead). **F**: In contrast, staining of P17O_2 retinas revealed almost no staining along either plexiform layer of the retina, and numerous F4/80$^+$ cells located within the neovascular tufts (arrows). **G**: Fluorescein angiography combined with F4/80 immunostaining demonstrates the intimate relationship between microglia and macrophages (red) and vessels (green) in the neovascular tufts (arrows). Magnification 400x.

(Figure 5A). Cells staining positive for BrdU were mainly localized to blood vessels (Figure 5A, arrows). Although an occasional F4/80$^+$ cell appeared to be co-localized with BrdU, many MG/MAC remained localized in the IPL and OPL (Figure 5A, arrowheads). The P17O_2 retinas demonstrated intense BrdU uptake by cells along the superficial retina and neovascular tufts (Figure 5B,C, arrows). The MG/MAC in the same sections were localized to the IPL and neovascular tufts (Figure 5B,C, arrowheads). Most of the F4/80$^+$ and BrdU$^+$ cells did not overlap; however, a small subset of BrdU-positive cells appeared to be surrounded by F4/80 cells. Therefore, proliferation of a small subset of F4/80$^+$ cells could not be totally excluded because of the close proximity of the two immunolabeled cells (Figure 5B, asterisk). P17 room air control retinas showed normal microglia staining and almost no positive BrdU-staining cells (data not shown).

P21O_2 retinas exhibited fewer mitotically active cells as compared to P14O_2 and P17O_2 (Figure 5D). Positive BrdU cells appeared to be adjacent to disrupted regions along the INL and the ONL interface (Figure 5D, arrows). Positive BrdU cells were distinctly not F4/80$^+$. However, the regions of retinal disruption were commonly associated with MG/MAC in the outer layers of the retina (Figure 5D, arrowheads), correlating with the findings of MG/MAC in the deep layers of the retinal whole mounts (Figure 4D,F).

Retinal expression of CCL2 mRNA: In order to determine if there is a specific cytokine or chemokine that is responsible for recruitment of MG/MAC into the retina, we ex-

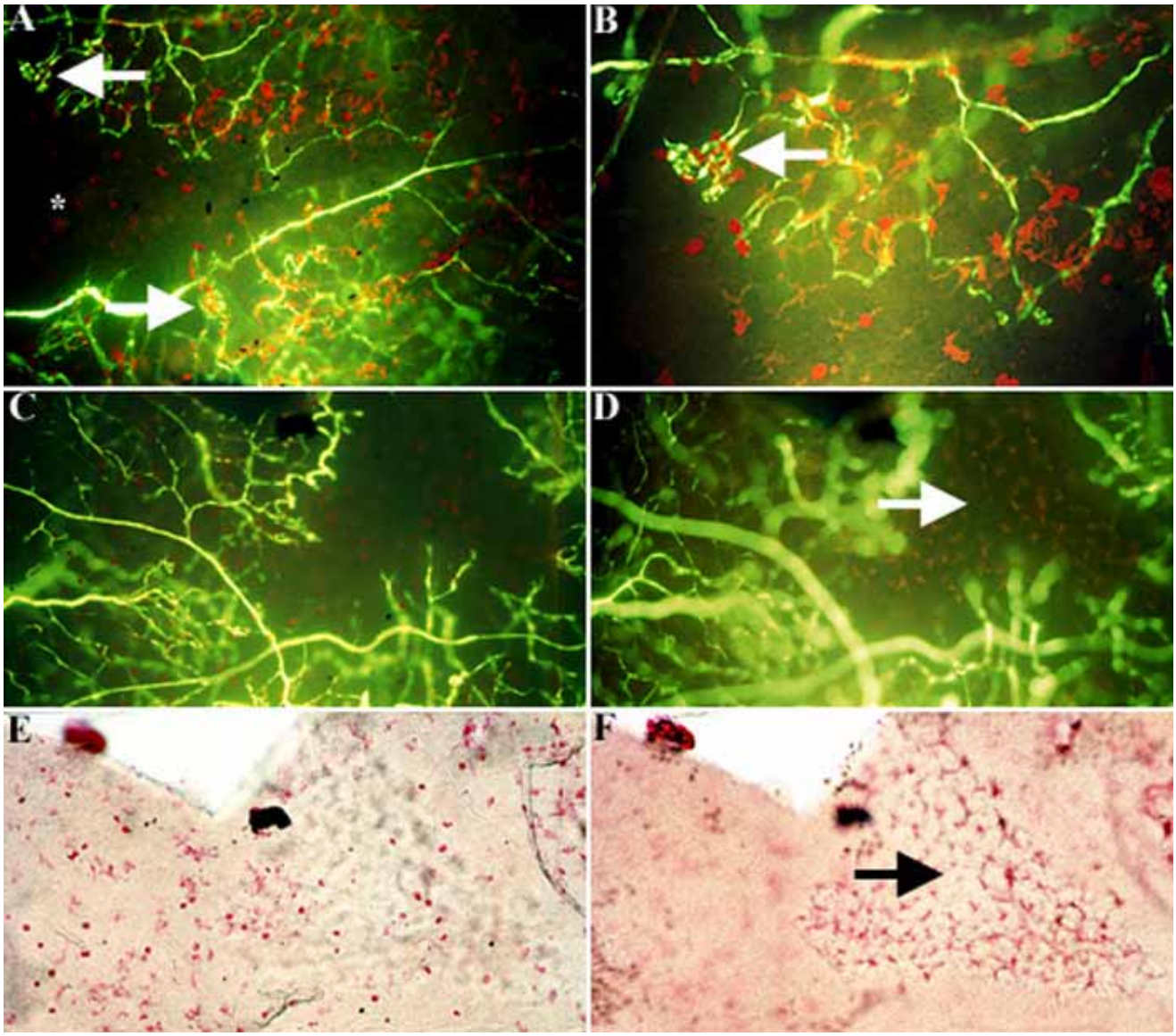

Figure 4. Microglia and macrophages localization in P21O_2 retinas. In the P21O_2 central retina, microglia and macrophages (red) continue to be primarily localized to vascular and avascular transition regions (**A**, asterisk) and neovascular tufts (**A**, arrow). Higher magnification (**A**, arrow) again reveals the intimate relationship between microglia and macrophages (MG/MAC) and neovascular tufts (**B**, arrow). While in the peripheral retina, MG/MAC are also localized to the superficial vascular network of the retina (**C**,**E**). However, in the deep vascular network MG/MAC are localized in areas corresponding to the avascular region (**D**,**F**, arrows). Magnification 100x (**A**), 200x (**B**-**F**).

amined mRNA extracted at various times from retinal tissue by RT-PCR. Semiquantatitive RT-PCR demonstrated that the expression of GM-CSF was not observed in the neonatal retina at any time, while M-CSF was constitutively expressed at all times (data not shown). However, quantitative real time RT-PCR analysis revealed a significant increase in CCL2 gene expression in hyperoxia-injured retinas as compared to room air control times on P14 and P17 (Figure 6). Samples were run on a gel to confirm product size (data not shown). These findings suggest that CCL2 could serve as a chemotactic factor for macrophage influx into the retina in this disease model. A primer pair for a constitutively expressed gene, β-actin, was run for each sample as a loading control.

DISCUSSION

In order to evaluate the contribution of microglia and macrophages in ischemic retinopathies, we examined the temporal and spatial expression of MG/MAC in the mouse model of oxygen-induced retinopathy. The resident microglia exhibited an activated morphology and migrated to the inner ischemic retina during the early times of relative hypoxia on $P14O_2$. Additionally, there was a marked increase (5 fold, $p<0.001$) in the number of $F4/80^+$ MG/MAC in the hyperoxia-injured retinas on P17 and P21 as compared to control retinas, corresponding to the peak days of retinal NV in this model. MG/MAC were localized to areas of NV, revealing an intimate relationship between MG/MAC and neovascular tufts on P17 and P21. Mouse retinal MG and infiltrating MAC share all available immunological surface markers, and it is not possible to distinguish between the two cell populations [33,37,38]. Double labeling with BrdU revealed that most of the proliferating cells were not labeled with F4/80, suggesting that the increased numbers of MG/MAC was related to infiltration of blood-borne macrophages. In addition, the MG/MAC are localized to the outer nuclear layer on $P21O_2$, suggesting a possible interaction with dying and apoptotic neurons, in contrast to interactions with the retinal vasculature. An increase in CCL2 mRNA expression was observed in oxygen-injured retinas as compared to room air controls. This suggests that CCL2 is likely serving a chemoattractant function for the infiltrating macrophages accounting for the increased numbers of $F4/80^+$ cells observed in the retinas on $P17O_2$ and $P21O_2$ [16-18].

There are several studies that demonstrate an angiogenic function for MG/MAC. This suggests a potential role for the activated MG and infiltrating MAC observed in these studies could be the release of direct and indirect angiogenic cytokines. A study examining neural allografts suggested that host microglia played an active role in promoting graft NV [39]. During the phase of graft development and NV, microglia were often localized in close proximity to ingrowing blood vessels, similar to that observed in our studies. MAC have been recognized for their angiogenic potential since the initial report in 1977 by Polverini et al. [40]. MAC are capable of releasing VEGF and have been linked to inflammatory NV and tumor angiogenesis [19,20,41,42]. MAC expression of tumor necrosis factor α (TNF-α) and VEGF has also been observed in choroidal neovascular membranes, suggesting that MAC can directly contribute to choroidal NV. In addition, TNF-α from macrophages can induce the release of VEGF from retinal pigment epithelial cells (RPE), providing an indirect angiogenic

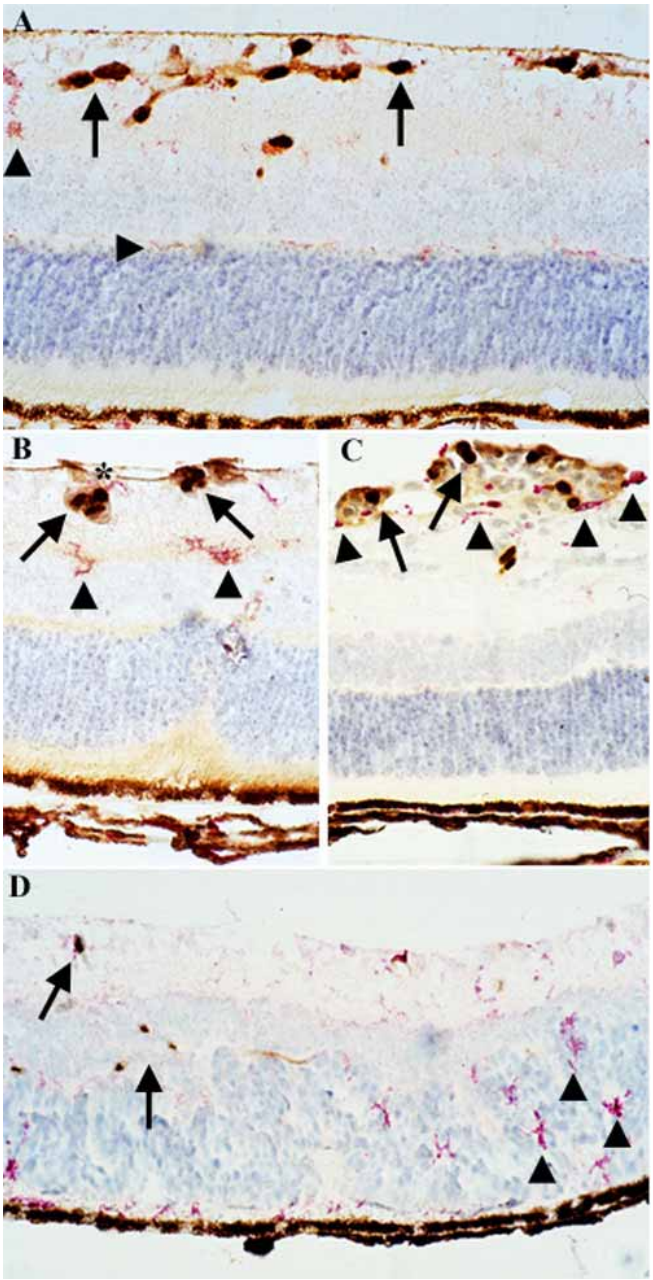

Figure 5. Retinal cell proliferation in oxygen-induced retinopathy. $P14O_2$ retinas (**A**) showed an increase in $BrdU^+$ nuclei (brown, arrows) following oxygen-induced injury, with $F4/80^+$ cells (red, arrowheads) localized to the outer plexiform layer, inner plexiform layer, and ganglion cell layer (GCL). $P17O_2$ retinal cross sections stained for F4/80 and BrdU shows rare co-localization (asterisk) of microglia and macrophages (MG/MAC; arrowheads) and proliferating nuclei (arrows; **B**,**C**). $P21O_2$ retinal cross sections (**D**) showed that MG/MAC located in deeper nuclear layers of the retina (arrowheads) did not correspond to those cells that are actively proliferating ($BrdU^+$, arrows).

stimulus [21,43]. Providing further evidence of the potential role that macrophages can play in NV, laser-induced choroidal NV was reduced in mice that had selective depletion of MAC with liposomal clodronate [44,45]. Furthermore, this reduction in the choroidal NV correlated with decreased VEGF protein levels as well as a decreased number of infiltrating macrophages [45].

In addition to its role as a MAC chemoattractant, CCL2 can also act as a direct angiogenic factor. The pro-angiogenic effects of CCL2 are not limited to the recruitment of macrophages but also are a result of direct activation of CCR2 (CCL2 receptor) that are localized to EC [46]. A recent study has shown a direct pro-angiogenic effect of CCL2 in a model of corneal angiogenesis [47]. Retinal glial cells in vitro have been shown to be a source of CCL2, hence the local retinal production of CCL2 from glial cells could be a direct factor in the angiogenic response in the mouse model of oxygen-induced retinopathy [48]. Consistent with this possibility, studies by Yoshida et al. [24] revealed that CCL2 is localized to the retinal ganglion cell layer and INL in the ischemic retina, regions of the retina that exhibit profound angiogenesis between $P14O_2$ and $P17O_2$ in this model [24]. However, intravitreal injection of a neutralizing antibody to CCL2 failed to reduce preretinal NV in the mouse model of oxygen-induced retinopathy unless combined with a neutralizing antibody to monocyte infiltrating protein 1-α (MIP-1α). Hence, the potential angiogenic effect of CCL2 in this model appears to be complex, possibly relating to: (1) the recruitment of pro-angiogenic macrophages, (2) a direct angiogenic effect, or (3) an interaction with other cytokines.

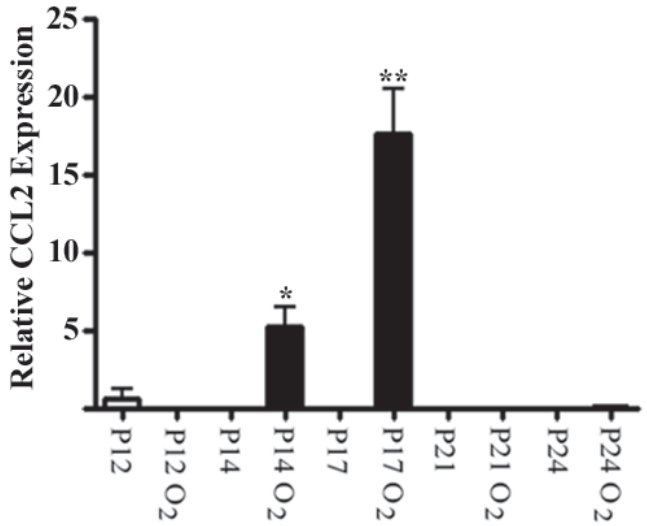

Figure 6. CCL2 mRNA expression in oxygen-induced retinopathy. Quantification of real-time readings of reverse transcriptase polymerase chain reaction products for relative CCL2 expression normalized to β-actin. Results are expressed as mean±SEM as analyzed by one-way ANOVA, followed by Tukey's multiple comparison post-test; a single asterisk indicates $p<0.05$ and a double asterisk indicates $p<0.001$.

In contrast to an angiogenic role for MG/MAC, there are likely alternative functions for these cells in their response to ischemic retinopathy, depending on the temporal phase of the injury. A recent study has suggested that MAC recruited early to injury sites tend to exacerbate the process, while late arriving MAC promoted recovery through apoptosis [49]. In the model of laser-induced choroidal NV infiltration of ocular MAC peaks prior to the onset of NV consistent with a pro-angiogenic role [22]. In contrast, the large influx of $F4/80^+$ cells continue to migrate into the retina during the phase of vascular tuft regression ($P18O_2$-$P21O_2$) in the model of oxygen-induced retinopathy. Previous studies using Fas-ligand deficient mice revealed that EC apoptosis plays a major role in the vascular tuft regression observed in this model [9,10]. MG/MAC have the potential to contribute to this vascular tuft regression through their phagocytic and pro-apoptotic functions. Similar to our studies in the retina, MG are activated locally and hematogenous MAC are recruited to the areas of injury in other models of central nervous system (CNS) injury [29,30,50]. The functions of MG/MAC delineated in these studies of the brain and eye include phagocytosis of dead cells, secretion of cytokines, antigen presentation, and induction of apoptosis [51,52]. Microglia are capable of releasing nerve growth factor and TNF-α, which can induce apoptosis in adjacent cells [25,53]. Activated macrophages can induce apoptosis in target cells through cell surface Fas-ligand and TNF-α [26,27,54]. As previously described, Fas-Fas-ligand interactions are involved with tuft regression in this model. In addition, TNF-α is also capable of mediating retinal EC cell death during inflammatory states, limiting NV during tissue ischemia [55-57]. MG/MAC have also been shown to exhibit increased expression of TNF-α in oxygen-exposed retinas as compared to room air control retinas. In addition, TNF-receptor-deficient mice also exhibit a prolonged neovascular response in the model of oxygen-induced retinopathy, with an associated decrease in EC apoptosis in the neovascular tufts, further supporting a role for TNF-α in vascular tuft regression [58]. Finally, the seminal work by Lang and colleagues demonstrated that MAC are required for EC death during the regression of the ocular capillaries in normal eye development [28,59,60], providing further evidence supporting the notion that MG/MAC are capable of pro-apoptotic functions in addition to their well characterized pro-angiogenic properties. We also have preliminary data that demonstrates decreased apoptosis within the NV tufts in $CCL2^{-/-}$ knockout mice at $P17O_2$. This was associated with a decrease in the number of infiltrating $F4/80^+$ cells into the injured retina [61]. Hence, it appears that MG/MAC has the potential to limit retinal NV by inducing apoptosis in adjacent EC, and our studies reveal an intimate relationship between the MG/MAC and EC localized in the neovascular tuft.

In addition to the co-localization of MG/MAC with retinal vessels in the oxygen-injured retinas on $P17O_2$ and $P21O_2$, we observed regions of severe disruption in the ONL that were also associated with an influx of MG/MAC on $P21O_2$. The disrupted regions were associated with residual avascular ar-

eas and are likely the most hypoxic regions of the retina. Previous studies suggested that MG/MAC target areas of focal ischemia in the retina and brain and can serve multiple roles, including pro-apoptotic, phagocytic, and neuroprotection [31,51,62,63]. Microglia are also capable of eliminating injured neurons, thus facilitating the death of neurons that are destined to die [64,65]. However, we have previously reported that the peak rate of apoptosis in the neural retina occurs at $P17O_2$ in the model of oxygen-induced retinopathy [10]. This suggests that photoreceptor apoptosis on $P17O_2$ likely leads to the disruption that we observed in $P21O_2$ retinas, having preceded the influx of MG/MAC to the disrupted regions. Therefore, in contrast to the proposed pro-apoptotic role for MG/MAC in vascular tuft EC death, in the neural retina the MG/MAC are less likely the initiators of neuron cell death, but rather are likely serving a phagocytic role. MG have been shown to express several scavenger receptors that are involved with phagocytosis of apoptotic cells and removal of cellular debris (membranes, myelin, and outer rod segments) [66]. An additional role for MG/MAC recruited to the ischemic retina could be to modify the extent of tissue damage by promoting neuron repair through the release of neuotrophic factors [51].

In summary, we have shown the temporal and spatial distribution of MG/MAC in this model of ischemic retinopathy. Potential functions of these cells include providing angiogenic signals to potentiate neovascular tuft formation, apoptotic induction to decrease retinal NV, modulation of the neuronal response. Studies using $CCL2^{-/-}$ mice in conjunction with MAC depletion studies will help clarify the contribution of MG/MAC to ischemic retinopathies.

ACKNOWLEDGEMENTS

This project was supported by NEI EY011548 (MRP), Research to Prevent Blindness, and the Medical Research Foundation of Oregon (MRP).

REFERENCES

1. Recchia FM, Capone A Jr. Contemporary understanding and management of retinopathy of prematurity. Retina 2004; 24:283-92.
2. Phelps DL. Retinopathy of prematurity. Pediatr Clin North Am 1993; 40:705-14.
3. Smith LE, Wesolowski E, McLellan A, Kostyk SK, D'Amato R, Sullivan R, D'Amore PA. Oxygen-induced retinopathy in the mouse. Invest Ophthalmol Vis Sci 1994; 35:101-11.
4. Penn JS, Tolman BL, Lowery LA. Variable oxygen exposure causes preretinal neovascularization in the newborn rat. Invest Ophthalmol Vis Sci 1993; 34:576-85.
5. Carmeliet P. Mechanisms of angiogenesis and arteriogenesis. Nat Med 2000; 6:389-95.
6. Pierce EA, Avery RL, Foley ED, Aiello LP, Smith LE. Vascular endothelial growth factor/vascular permeability factor expression in a mouse model of retinal neovascularization. Proc Natl Acad Sci U S A 1995; 92:905-9.
7. Smith LE, Shen W, Perruzzi C, Soker S, Kinose F, Xu X, Robinson G, Driver S, Bischoff J, Zhang B, Schaeffer JM, Senger DR. Regulation of vascular endothelial growth factor-dependent retinal neovascularization by insulin-like growth factor-1 receptor. Nat Med 1999; 5:1390-5.
8. Carmeliet P. Angiogenesis in health and disease. Nat Med 2003; 9:653-60.
9. Barreiro R, Schadlu R, Herndon J, Kaplan HJ, Ferguson TA. The role of Fas-FasL in the development and treatment of ischemic retinopathy. Invest Ophthalmol Vis Sci 2003; 44:1282-6.
10. Davies MH, Eubanks JP, Powers MR. Increased retinal neovascularization in Fas ligand-deficient mice. Invest Ophthalmol Vis Sci 2003; 44:3202-10.
11. Chen L, Yang P, Kijlstra A. Distribution, markers, and functions of retinal microglia. Ocul Immunol Inflamm 2002; 10:27-39.
12. Egensperger R, Maslim J, Bisti S, Hollander H, Stone J. Fate of DNA from retinal cells dying during development: uptake by microglia and macroglia (Muller cells). Brain Res Dev Brain Res 1996; 97:1-8.
13. Yang P, de Vos AF, Kijlstra A. Macrophages in the retina of normal Lewis rats and their dynamics after injection of lipopolysaccharide. Invest Ophthalmol Vis Sci 1996; 37:77-85.
14. Rossi D, Zlotnik A. The biology of chemokines and their receptors. Annu Rev Immunol 2000; 18:217-42.
15. Lira SA. Genetic approaches to study chemokine function. J Leukoc Biol 1996; 59:45-52.
16. Lu B, Rutledge BJ, Gu L, Fiorillo J, Lukacs NW, Kunkel SL, North R, Gerard C, Rollins BJ. Abnormalities in monocyte recruitment and cytokine expression in monocyte chemoattractant protein 1-deficient mice. J Exp Med 1998; 187:601-8.
17. Chae P, Im M, Gibson F, Jiang Y, Graves DT. Mice lacking monocyte chemoattractant protein 1 have enhanced susceptibility to an interstitial polymicrobial infection due to impaired monocyte recruitment. Infect Immun 2002; 70:3164-9.
18. Tesch GH, Schwarting A, Kinoshita K, Lan HY, Rollins BJ, Kelley VR. Monocyte chemoattractant protein-1 promotes macrophage-mediated tubular injury, but not glomerular injury, in nephrotoxic serum nephritis. J Clin Invest 1999; 103:73-80.
19. Barbera-Guillem E, Nyhus JK, Wolford CC, Friece CR, Sampsel JW. Vascular endothelial growth factor secretion by tumor-infiltrating macrophages essentially supports tumor angiogenesis, and IgG immune complexes potentiate the process. Cancer Res 2002; 62:7042-9.
20. Cursiefen C, Chen L, Borges LP, Jackson D, Cao J, Radziejewski C, D'Amore PA, Dana MR, Wiegand SJ, Streilein JW. VEGF-A stimulates lymphangiogenesis and hemangiogenesis in inflammatory neovascularization via macrophage recruitment. J Clin Invest 2004; 113:1040-50.
21. Oh H, Takagi H, Takagi C, Suzuma K, Otani A, Ishida K, Matsumura M, Ogura Y, Honda Y. The potential angiogenic role of macrophages in the formation of choroidal neovascular membranes. Invest Ophthalmol Vis Sci 1999; 40:1891-8.
22. Tsutsumi C, Sonoda KH, Egashira K, Qiao H, Hisatomi T, Nakao S, Ishibashi M, Charo IF, Sakamoto T, Murata T, Ishibashi T. The critical role of ocular-infiltrating macrophages in the development of choroidal neovascularization. J Leukoc Biol 2003; 74:25-32.
23. Rungger-Brandle E, Dosso AA, Leuenberger PM. Glial reactivity, an early feature of diabetic retinopathy. Invest Ophthalmol Vis Sci 2000; 41:1971-80.
24. Yoshida S, Yoshida A, Ishibashi T, Elner SG, Elner VM. Role of MCP-1 and MIP-1alpha in retinal neovascularization during postischemic inflammation in a mouse model of retinal neovascularization. J Leukoc Biol 2003; 73:137-44.
25. Frade JM, Barde YA. Microglia-derived nerve growth factor causes cell death in the developing retina. Neuron 1998; 20:35-41.

26. Boyle JJ, Bowyer DE, Weissberg PL, Bennett MR. Human blood-derived macrophages induce apoptosis in human plaque-derived vascular smooth muscle cells by Fas-ligand/Fas interactions. Arterioscler Thromb Vasc Biol 2001; 21:1402-7.
27. Saio M, Radoja S, Marino M, Frey AB. Tumor-infiltrating macrophages induce apoptosis in activated CD8(+) T cells by a mechanism requiring cell contact and mediated by both the cell-associated form of TNF and nitric oxide. J Immunol 2001; 167:5583-93.
28. Lang R, Lustig M, Francois F, Sellinger M, Plesken H. Apoptosis during macrophage-dependent ocular tissue remodelling. Development 1994; 120:3395-403.
29. Ivacko J, Szaflarski J, Malinak C, Flory C, Warren JS, Silverstein FS. Hypoxic-ischemic injury induces monocyte chemoattractant protein-1 expression in neonatal rat brain. J Cereb Blood Flow Metab 1997; 17:759-70.
30. Gehrmann J, Banati RB, Wiessner C, Hossmann KA, Kreutzberg GW. Reactive microglia in cerebral ischaemia: an early mediator of tissue damage? Neuropathol Appl Neurobiol 1995; 21:277-89.
31. Schroeter M, Jander S, Huitinga I, Stoll G. CD8+ phagocytes in focal ischemia of the rat brain: predominant origin from hematogenous macrophages and targeting to areas of pannecrosis. Acta Neuropathol (Berl) 2001; 101:440-8.
32. Connolly SE, Hores TA, Smith LE, D'Amore PA. Characterization of vascular development in the mouse retina. Microvasc Res 1988; 36:275-90.
33. Austyn JM, Gordon S. F4/80, a monoclonal antibody directed specifically against the mouse macrophage. Eur J Immunol 1981; 11:805-15.
34. Ellwart J, Dormer P. Effect of 5-fluoro-2'-deoxyuridine (FdUrd) on 5-bromo-2'-deoxyuridine (BrdUrd) incorporation into DNA measured with a monoclonal BrdUrd antibody and by the BrdUrd/Hoechst quenching effect. Cytometry 1985; 6:513-20.
35. Gruffat D, Piot C, Durand D, Bauchart D. Comparison of four methods for isolating large mRNA: apolipoprotein B mRNA in bovine and rat livers. Anal Biochem 1996; 242:77-83.
36. Hume DA, Perry VH, Gordon S. Immunohistochemical localization of a macrophage-specific antigen in developing mouse retina: phagocytosis of dying neurons and differentiation of microglial cells to form a regular array in the plexiform layers. J Cell Biol 1983; 97:253-7.
37. Imai Y, Ibata I, Ito D, Ohsawa K, Kohsaka S. A novel gene iba1 in the major histocompatibility complex class III region encoding an EF hand protein expressed in a monocytic lineage. Biochem Biophys Res Commun 1996; 224:855-62.
38. Broderick C, Hoek RM, Forrester JV, Liversidge J, Sedgwick JD, Dick AD. Constitutive retinal CD200 expression regulates resident microglia and activation state of inflammatory cells during experimental autoimmune uveoretinitis. Am J Pathol 2002; 161:1669-77.
39. Pennell NA, Streit WJ. Colonization of neural allografts by host microglial cells: relationship to graft neovascularization. Cell Transplant 1997; 6:221-30.
40. Polverini PJ, Cotran PS, Gimbrone MA Jr, Unanue ER. Activated macrophages induce vascular proliferation. Nature 1977; 269:804-6.
41. Xiong M, Elson G, Legarda D, Leibovich SJ. Production of vascular endothelial growth factor by murine macrophages: regulation by hypoxia, lactate, and the inducible nitric oxide synthase pathway. Am J Pathol 1998; 153:587-98.
42. Crowther M, Brown NJ, Bishop ET, Lewis CE. Microenvironmental influence on macrophage regulation of angiogenesis in wounds and malignant tumors. J Leukoc Biol 2001; 70:478-90.
43. Grossniklaus HE, Ling JX, Wallace TM, Dithmar S, Lawson DH, Cohen C, Elner VM, Elner SG, Sternberg P Jr. Macrophage and retinal pigment epithelium expression of angiogenic cytokines in choroidal neovascularization. Mol Vis 2002; 8:119-26.
44. Espinosa-Heidmann DG, Suner IJ, Hernandez EP, Monroy D, Csaky KG, Cousins SW. Macrophage depletion diminishes lesion size and severity in experimental choroidal neovascularization. Invest Ophthalmol Vis Sci 2003; 44:3586-92.
45. Ambati BK, Joussen AM, Kuziel WA, Adamis AP, Ambati J. Inhibition of corneal neovascularization by genetic ablation of CCR2. Cornea 2003; 22:465-7.
46. Salcedo R, Ponce ML, Young HA, Wasserman K, Ward JM, Kleinman HK, Oppenheim JJ, Murphy WJ. Human endothelial cells express CCR2 and respond to MCP-1: direct role of MCP-1 in angiogenesis and tumor progression. Blood 2000; 96:34-40.
47. Goede V, Brogelli L, Ziche M, Augustin HG. Induction of inflammatory angiogenesis by monocyte chemoattractant protein-1. Int J Cancer 1999; 82:765-70.
48. Yoshida S, Yoshida A, Ishibashi T. Induction of IL-8, MCP-1, and bFGF by TNF-alpha in retinal glial cells: implications for retinal neovascularization during post-ischemic inflammation. Graefes Arch Clin Exp Ophthalmol 2004; 242:409-13.
49. Friedman SL. Mac the knife? Macrophages- the double-edged sword of hepatic fibrosis. J Clin Invest 2005; 115:29-32.
50. Rogers J, Strohmeyer R, Kovelowski CJ, Li R. Microglia and inflammatory mechanisms in the clearance of amyloid beta peptide. Glia 2002; 40:260-9.
51. Streit WJ. Microglia as neuroprotective, immunocompetent cells of the CNS. Glia 2002; 40:133-9.
52. Thomas WE. Brain macrophages: evaluation of microglia and their functions. Brain Res Brain Res Rev 1992; 17:61-74.
53. Rao NA, Kimoto T, Zamir E, Giri R, Wang R, Ito S, Pararajasegaram G, Read RW, Wu GS. Pathogenic role of retinal microglia in experimental uveoretinitis. Invest Ophthalmol Vis Sci 2003; 44:22-31.
54. Wang T, Dong C, Stevenson SC, Herderick EE, Marshall-Neff J, Vasudevan SS, Moldovan NI, Michler RE, Movva NR, Goldschmidt-Clermont PJ. Overexpression of soluble fas attenuates transplant arteriosclerosis in rat aortic allografts. Circulation 2002; 106:1536-42.
55. Duffield JS, Erwig LP, Wei X, Liew FY, Rees AJ, Savill JS. Activated macrophages direct apoptosis and suppress mitosis of mesangial cells. J Immunol 2000; 164:2110-9.
56. Koizumi K, Poulaki V, Doehmen S, Welsandt G, Radetzky S, Lappas A, Kociok N, Kirchhof B, Joussen AM. Contribution of TNF-alpha to leukocyte adhesion, vascular leakage, and apoptotic cell death in endotoxin-induced uveitis in vivo. Invest Ophthalmol Vis Sci 2003; 44:2184-91.
57. Ashton AW, Ware GM, Kaul DK, Ware JA. Inhibition of tumor necrosis factor alpha-mediated NFkappaB activation and leukocyte adhesion, with enhanced endothelial apoptosis, by G protein-linked receptor (TP) ligands. J Biol Chem 2003; 278:11858-66.
58. Ilg RC, Davies MH, Powers MR. Altered retinal neovascularization in TNF receptor-deficient mice. Curr Eye Res 2005; 30:1003-13.
59. Diez-Roux G, Argilla M, Makarenkova H, Ko K, Lang RA. Macrophages kill capillary cells in G1 phase of the cell cycle during programmed vascular regression. Development 1999; 126:2141-7.

60. Lang RA, Bishop JM. Macrophages are required for cell death and tissue remodeling in the developing mouse eye. Cell 1993; 74:453-62.
61. Davies MH, Powers MR. MCP-1 deficient mice exhibit a prolonged neovascular response in a mouse model of oxygen-induced retinopathy. ARVO Annual Meeting; 2005 May 1-5; Fort Lauderdale (FL).
62. Roque RS, Rosales AA, Jingjing L, Agarwal N, Al-Ubaidi MR. Retina-derived microglial cells induce photoreceptor cell death in vitro. Brain Res 1999; 836:110-9.
63. Roque RS, Imperial CJ, Caldwell RB. Microglial cells invade the outer retina as photoreceptors degenerate in Royal College of Surgeons rats. Invest Ophthalmol Vis Sci 1996; 37:196-203.
64. Thanos S. Sick photoreceptors attract activated microglia from the ganglion cell layer: a model to study the inflammatory cascades in rats with inherited retinal dystrophy. Brain Res 1992; 588:21-8.
65. Streit WJ. Microglia and macrophages in the developing CNS. Neurotoxicology 2001; 22:619-24.
66. Husemann J, Loike JD, Anankov R, Febbraio M, Silverstein SC. Scavenger receptors in neurobiology and neuropathology: their role on microglia and other cells of the nervous system. Glia 2002; 40:195-205.

The print version of this article was created on 10 May 2006. This reflects all typographical corrections and errata to the article through that date. Details of any changes may be found in the online version of the article.